H(curl) Auxiliary Mesh Preconditioning

T.V. Kolev, J.E. Pasciak, P.S. Vassilevski

September 7, 2006

Disclaimer

H(curl) **AUXILIARY MESH PRECONDITIONING**

TZANIO V. KOLEV, JOSEPH E. PASCIAK, AND PANAYOT S. VASSILEVSKI

ABSTRACT. This paper analyzes a two–level preconditioning scheme for $\mathbf{H}$(curl) bilinear forms. The scheme utilizes an auxiliary problem on a related mesh that is more amenable for constructing optimal order multigrid methods. More specifically, we analyze the case when the auxiliary mesh only approximately covers the original domain. The latter assumption is important since it allows for easy construction of nested multilevel spaces on regular auxiliary meshes. Numerical experiments in both two and three space dimensions illustrate the optimal performance of the method.

1. INTRODUCTION

This paper analyzes a two–level preconditioning scheme for the H(curl) problem previously developed for elliptic finite element problems (cf., [5], [20], [7]). A main motivation for such an approach is to be able to solve finite element problems posed on unstructured meshes, by methods available for discretizations of the same PDE on a related auxiliary mesh for which preconditioners (for example of multigrid type) are easier to construct. The two–level auxiliary mesh scheme, in combination with a related domain embedding technique (or "fictitious" domain methods, going back as early as to [9], [3]) may be seen as a more practical motivation for the kind of study we have taken in the present paper. The specific problem we consider comes from Maxwell equations and leads to a bilinear form on the space $\mathbf{H}(\Omega; \text{curl})$ for a 3D polyhedral domain Ω. For simplicity, we take Ω to be simply connected with a connected boundary. Since the resulting form is not equivalent to a standard second order elliptic one, the analysis we present is a bit more involved, a main part of which is to establish that a discrete de Rham diagram commutes for two sequences of non-related finite element spaces and the natural interpolation operators associated with them.

Our result is closely related to those of a recent paper [14] dealing with the same topic. The difference is that our analysis is more general; in particular, it applies to the lowest order Nédélec space whereas the result in [14] substantially relies on the fact that the auxiliary Nédélec space contains an $\mathbf{H}^1$–conforming subspace. Another difference is that we provide experiments in three dimensions. A main ingredient in the implementation is the construction of the mapping $\mathbf{\Pi}_h^Q$ that relates the auxiliary mesh Nédélec space $\mathbf{Q}_H$ with the original one $\mathbf{Q}_h$ (for more details see Section 3).

As it turned out, the newly proposed multilevel method by Hiptmair and Xu in [15] utilizes a similar operator that however relates a $\mathbf{H}^1$–conforming space $\mathbf{S}_h$ on the same mesh with the original Nédélec space $\mathbf{Q}_h$. That is, the method in [15] does not require remeshing the domain; it uses a $\mathbf{H}^1$–conforming auxiliary space on the original mesh, instead. Our present implementation of $\mathbf{\Pi}_h^Q$ is somewhat involved since it is computed as a mapping from a finite element space defined on a different (auxiliary) mesh into a space on the original mesh. However, it enabled us to easily implement and test the performance, both in serial and in parallel (see [17] and [16]) of a modified version of the method in [15]. Combining both approaches (from the present paper and [15]) we can allow auxiliary meshes that do not completely cover the original domain and either use auxiliary Nédélec spaces or auxiliary $\mathbf{H}^1$–conforming spaces on them to construct efficient auxiliary mesh/space preconditioners.

The remainder of the paper is structured as follows. In Section 2 we pose the problem, define the two–level preconditioning scheme in general terms, and give details about the auxiliary mesh and space. In Section 3 the main properties of the mapping $\mathbf{\Pi}_h^Q$ are stated. Then, in Section 4 the so–called Hiptmair smoother is reviewed. Section 5 contains the proof of our main theorem, The commuting property of the discrete de Rham diagram and a related L^2-stability of the natural interpolation operators associated with it, are the main subject of Section 6. Finally, numerical experiments both in two and three space dimensions illustrating the theory are presented in Section 7.

2. The $\mathbf{H}(\mathrm{curl})$ problem and its two–level preconditioning

We shall denote $\mathbf{L}^2(\Omega)$ to be the space of vector functions on Ω whose components are in $L^2(\Omega)$. For scalar and vector functions, we shall use $(\cdot, \cdot)$ to denote the inner product both in $\mathbf{L}^2(\Omega)$ and $L^2(\Omega)$. The corresponding norm will be denoted $\| \cdot \|_0$ while the norm on $H^1(\Omega)$ and $\mathbf{H}^1(\Omega) \equiv H^1(\Omega)^3$ will be denoted $\| \cdot \|_1$.

We consider the following bilinear form

$$A(\mathbf{u}, \mathbf{v}) = (\mathbf{u}, \mathbf{v}) + (\nabla \times \mathbf{u}, \nabla \times \mathbf{v}),$$

for functions $\mathbf{u}, \mathbf{v}$ in $\mathbf{H}(\Omega; \mathrm{curl})$.

We assume that Ω is triangulated by a quasi-uniform mesh $\mathcal{T}_h$ consisting of tetrahedrons of size h. Let P_r be the space of polynomials of degree at most r and $\mathbf{P}_r$ denote P_r^3. We associate with $\mathcal{T}_h$ the $\mathbf{H}_0(\Omega; \mathrm{curl})$–conforming Nédélec space $\mathbf{Q}_h$ of order r. On each element $K \in \mathcal{T}_h$, functions in $\mathbf{Q}_h$ are polynomials of degree at most $r + 1$ of the form

$$\mathbf{P}(\mathbf{x}) = \mathbf{Q}(\mathbf{x}) + \mathbf{R}(\mathbf{x})$$

where $\mathbf{Q} \in \mathbf{P}_r$ and $\mathbf{R}$ is a homogeneous vector polynomial of degree $r + 1$ satisfying $\mathbf{R} \cdot \mathbf{x} = 0$ for all $\mathbf{x} \in \mathbb{R}^3$.

The form $A(.,.)$ restricted to $\mathbf{Q}_h \times \mathbf{Q}_h$ defines a symmetric and positive definite operator A_h, i.e., for $\mathbf{v} \in \mathbf{Q}_h$, $A_h \mathbf{v}$ is the unique function in $\mathbf{Q}_h$ satisfying

$$(2.1) \qquad\qquad (A_h \mathbf{v}, \boldsymbol{\theta}) = A(\mathbf{v}, \boldsymbol{\theta}) \quad \text{for all } \boldsymbol{\theta} \in \mathbf{Q}_h.$$

Our goal in this paper is to construct a two-level preconditioner B_h for A_h which utilizes an auxiliary mesh $\mathcal{T}_H$ obtained by using a mesh whose elements consist of

the elements of a uniform mesh which are contained in Ω (see Figure 1). Such a mesh does not fit the domain Ω but is a reasonable approximation to it. Multilevel algorithms are easy to set up for this mesh if we take the original $H-$mesh to be a geometrically refined uniform grid. Let $\mathbf{Q}_H$ denote the Nédélec space associated with the mesh $\mathcal{T}_H$ of functions in $\mathbf{H}_0(\Omega_H; \mathrm{curl})$ where $\Omega_H = \cup T$, $T \in \mathcal{T}_H$, and $T \subset \Omega$. By extension by zero, we can consider functions in $\mathbf{Q}_H$ as a subset of $\mathbf{H}_0(\Omega; \mathrm{curl})$.
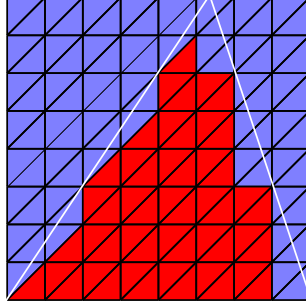

FIGURE 1. Example of an auxiliary mesh $\mathcal{T}_H$ (in red) embedded in the original triangular domain Ω.

We assume that the meshes $\mathcal{T}_h$ and $\mathcal{T}_H$ are roughly of the same size, i.e., $C_0 h \leq H \leq C_1 h$ and denote that with $h \simeq H$. Here and in the remainder of this paper, C, with or without subscript, denotes a generic positive constant which is independent of h.

The resulting preconditioner B_h involves smoothing on $\mathbf{Q}_h$ and an auxiliary preconditioner B_H for the problem on $\mathbf{Q}_H$ (see Remark 5.1). Specifically, the two–level operator B_h, is defined by

$$(2.2) \qquad B_h = R_h + \mathbf{\Pi}_h^Q B_H \left(\mathbf{\Pi}_h^Q \right)^T,$$

where R_h is the smoothing operator on $\mathbf{Q}_h$ and B_H denotes a multilevel preconditioner on $\mathbf{Q}_H$. Here $\mathbf{\Pi}_h^Q$ denotes the natural interpolation operator associated with the Nédélec space $\mathbf{Q}_h$ and $(\mathbf{\Pi}_h^Q)^T$ denotes its $\mathbf{L}^2(\Omega)$ adjoint. The construction and analysis of geometric multigrid preconditioners B_H for the problem on $\mathbf{Q}_H$ (when the mesh of $\mathcal{T}_H$ fills Ω) has been well researched [12, 11, 2, 13]. It results in an operator $B_H : \mathbf{Q}_H \to \mathbf{Q}_H$ satisfying

$$(2.3) \qquad c_0 A(\mathbf{v}, \mathbf{v}) \leq (B_H^{-1} \mathbf{v}, \mathbf{v}) \leq c_1 A(\mathbf{v}, \mathbf{v}) \quad \text{for all } \mathbf{v} \in \mathbf{Q}_H$$

with constants c_0, c_1 independent of H. We stress the fact that our result holds even when the elements of $\mathcal{T}_H$ do not fill Ω (but approximate it of order $H \simeq h$). Our numerical experiments clearly support these findings.

From (2.3) and the fact that B_h is an additive algorithm, the analysis of B_h reduces to that of the preconditioner with the exact solve on $\mathbf{Q}_H$, i.e.,

$$(2.4) \qquad \widetilde{B}_h = R_h + \mathbf{\Pi}_h^Q A_H^{-1} \left(\mathbf{\Pi}_h^Q \right)^T.$$

Here A_H is the operator corresponding to $A(\cdot, \cdot)$ on $\mathbf{Q}_H$ (analogous to (2.1)).

The following well known identity (cf., e.g., [19], Lemma 1 on p. 154) holds: For $\mathbf{v}_h \in \mathbf{Q}_h$,

$$(2.5) \qquad (\widetilde{B}_h^{-1}\mathbf{v}_h, \mathbf{v}_h) = \inf_{\mathbf{v}_h = \mathbf{w}_h + \boldsymbol{\Pi}_h^Q \mathbf{v}_H} \left\{ (R_h^{-1}\mathbf{w}_h, \mathbf{w}_h) + A_H(\mathbf{v}_H, \mathbf{v}_H) \right\}.$$

The infimum is taken over all decompositions of the above form with $\mathbf{w}_h \in \mathbf{Q}_h$ and $\mathbf{v}_H \in \mathbf{Q}_H$.

3. The analysis of $\boldsymbol{\Pi}_h^Q$.

In this section, we derive some properties of $\boldsymbol{\Pi}_h^Q$, specifically, we need to check how if behaves when applied to functions in $\mathbf{Q}_H$. Actually, we shall have to deal with all of the corresponding operators which appear in the de Rham sequence. Specifically, we denote by S_h the functions in $H_0^1(\Omega)$ whose restriction to $K \in \mathcal{T}_h$ are in P_r. We also denote the Raviart-Thomas space $\mathbf{R}_h$ to be the set of functions in $\mathbf{H}_0(\Omega; \mathrm{div})$ whose restriction to $K \in \mathcal{T}_h$ are polynomials of the form

$$\mathbf{P}(\mathbf{x}) = \mathbf{Q}(\mathbf{x}) + R(\mathbf{x})\mathbf{x}$$

where $\mathbf{Q} \in \mathbf{P}_r$ and R is a homogeneous polynomial of degree r. We then have the exact sequence

$$0 \longrightarrow S_h \xrightarrow{\nabla} \mathbf{Q}_h \xrightarrow{\nabla\times} \mathbf{R}_h.$$

The analogous spaces on the mesh $\mathcal{T}_H$ are denoted S_H, $\mathbf{Q}_H$ and $\mathbf{R}_H$. These have zero nodal components on the boundary of Ω_H and are extended by zero to Ω.

Along with the spaces S_h, $\mathbf{Q}_h$ and $\mathbf{R}_h$, there are natural interpolation operators (see, e.g., [8, 10]) Π_h^S, $\boldsymbol{\Pi}_h^Q$ and $\boldsymbol{\Pi}_h^R$. These operators are defined for sufficiently smooth functions, e.g., Π_h^S is defined on functions in $H^{1+s}(\Omega)$ for any $s > 0$. $\boldsymbol{\Pi}_h^Q$ is defined for functions $\mathbf{v} \in \mathbf{H}^s(\Omega)$ for $s > 1/2$ satisfying $\nabla \times \mathbf{v} \in \mathbf{L}^p(\Omega)$ for $p > 2$ [1]. Finally, $\boldsymbol{\Pi}_h^R$ is defined for functions $\mathbf{v} \in \mathbf{H}^s(\Omega)$ with $s > 0$ satisfying $\nabla \cdot \mathbf{v} \in L^p(\Omega)$ for $p > 2$.

From the above discussion, it is not clear that the interpolation operator $\boldsymbol{\Pi}_h^Q$ is even well defined on $\mathbf{Q}_H$. That this is the case is given by the following theorem whose proof appears later.

Theorem 3.1. *The interpolation operators Π_h^S, $\boldsymbol{\Pi}_h^Q$ and $\boldsymbol{\Pi}_h^R$ are well–defined on S_H, $\mathbf{Q}_H$ and $\mathbf{R}_H$. Furthermore, they are stable, respectively, in the $L^2(\Omega)$ and $\mathbf{L}^2(\Omega)$ norms on these spaces and the following diagram commutes:*

$$(3.1) \qquad
\begin{array}{ccccc}
S_H & \xrightarrow{\nabla} & \mathbf{Q}_H & \xrightarrow{\nabla\times} & \mathbf{R}_H \\
\Pi_h^S \downarrow & & \boldsymbol{\Pi}_h^Q \downarrow & & \boldsymbol{\Pi}_h^R \downarrow \\
S_h & \xrightarrow{\nabla} & \mathbf{Q}_h & \xrightarrow{\nabla\times} & \mathbf{R}_h
\end{array}$$

As a consequence one gets the following stability result:

Corollary 3.1. *For $\mathbf{u} \in \mathbf{Q}_H$,*

$$\|\nabla \times \boldsymbol{\Pi}_h^Q \mathbf{u}\|_0 = \|\boldsymbol{\Pi}_h^R(\nabla \times \mathbf{u})\|_0 \leq C\|\nabla \times \mathbf{u}\|_0,$$

that is, $\boldsymbol{\Pi}_h^Q$ is stable in the $\mathbf{H}(\Omega; \mathrm{curl})$-norm on $\mathbf{Q}_H$.

Remark 3.1. *The proof of the above theorem actually shows that,*

$$\|\mathbf{\Pi}_h^Q \mathbf{w}_H\|_{0,K} \le C\|\mathbf{w}_H\|_{0,\widehat{K}}, \quad \textit{for all } \mathbf{w}_H \in \mathbf{Q}_H.$$

and

$$\|\Pi_h^S v_H\|_{0,K} \le C\|v_H\|_{0,\widehat{K}}, \quad \textit{for all } v_H \in S_H.$$

Here K is a given element from $\mathcal{T}_h$ and $\widehat{K}$ is a union of $\mathcal{T}_H$ elements that intersect K.

Let v_H be in S_H. Set $\bar{v}_H$ be the mean value of v_H on $\widehat{K}$ if $\widehat{K} \cap \partial\Omega = \emptyset$, otherwise, set $\bar{v}_H = 0$. We note that

$$(3.2) \qquad \|v_H - \bar{v}_H\|_{0,\widehat{K}} \le Ch\|v_H\|_{1,\widehat{K}}.$$

Such inequalities for clusters $\widehat{K}$ which are star shaped with respect to a ball are given in [6]. A more general argument is given in [5]. We then have

$$\|v_H - \Pi_h^S v_H\|_{0,K} \le C\|v_H - \bar{v}_H\|_{0,K} + \|\pi_h^S(v_H - \bar{v}_H)\|_{0,K} \le Ch\|v_H\|_{1,\widehat{K}}$$

where we used the above remark and (3.2) for the last inequality. The inequality

$$\|v_H - \Pi_h^S v_H\|_0 \le Ch\|v_H\|_1$$

follows by summation. Finally, using the Clement projector and inverse inequalities gives

$$(3.3) \qquad \|v - \Pi_h^S v\|_0 + h\|\Pi_h^S v\|_1 \le Ch\|v\|_1 \quad \text{for all } v \in S_H.$$

This estimate is non-standard in that it fails to hold for general H^1 functions as the nodal values are not well defined there.

Also, if $\mathbf{z}_h \in \mathbf{S}_h \equiv S_h^3$ then

$$(3.4) \qquad \|\mathbf{z}_h - \mathbf{\Pi}_h^Q \mathbf{z}_h\|_0 \le Ch\|\mathbf{z}_h\|_1$$

and, for $K \in \mathcal{T}_h$,

$$(3.5) \qquad \|\mathbf{\Pi}_h^Q \mathbf{z}_h\|_{0,K} \le C\|\mathbf{z}_h\|_{0,K}.$$

The inequality (3.4) depends on $\mathbf{z}_h$ being piecewise polynomial on the h-mesh while (3.5) follows from a simple scaling argument. Finally, (3.4) and an inverse inequality (when applied to H) implies

$$(3.6) \qquad \|\mathbf{\Pi}_H^Q \mathbf{z}_H\|_{\mathbf{H}(\Omega;\mathrm{curl})} \le C\|\mathbf{z}_H\|_1 \quad \text{for all } \mathbf{z}_H \in \mathbf{S}_H.$$

4. The Hiptmair smoother

We can now define the so–called "Hiptmair" smoother. Let $\{\theta_j\}_{j=1}^M$ be a nodal basis for S_h and $\{\phi_k\}_{k=1}^N$ be the nodal basis for $\mathbf{Q}_h$. We consider the set $\{\Theta_i\} = \{\phi_j\} \cup \{\nabla\theta_j\}$ and define the one dimensional subspace $\mathbf{Q}_{h,i}$ to be the span of Θ_i, $i = 1, \ldots, N + M$. We let $Q_{h,i}$ and $P_{h,i}$ respectively denote the $\mathbf{L}^2(\Omega)$ and $A(\cdot, \cdot)$ projectors onto $\mathbf{Q}_{h,i}$.

The Hiptmair smoother is defined to be the additive smoother associated with these spaces, i.e.,

$$R_h = \sum_{i=1}^{N+M} A_{h,i}^{-1} Q_{h,i}.$$

Here $A_{h,i} : \mathbf{Q}_{h,i} \to \mathbf{Q}_{h,i}$ is defined by

$$(A_{h,i}v, w) = A(v, w) \quad \text{for } v, w \in \mathbf{Q}_{h,i}.$$

Similar to (2.5), we have the identity

$$(R_h^{-1}\mathbf{w}_h, \mathbf{w}_h) = \inf \left(\sum_{i=1}^{N} A(v_i, v_i) + \sum_{i=N+1}^{N+M} (\nabla p_i, \nabla p_i) \right).$$

Here $v_i \in \mathbf{Q}_{h,i}$, $i = 1, \ldots, N$, $\nabla p_i \in \mathbf{Q}_{h,i}$, $i = N + 1, \ldots, N + M$ and the infimum is taken over all such decompositions of $\mathbf{w}_h$. It follows from the limited overlap of nodal basis functions that

$$(4.1) \qquad\qquad A(\mathbf{w}_h, \mathbf{w}_h) \le C(R_h^{-1}\mathbf{w}_h, \mathbf{w}_h).$$

Now if $\mathbf{w}_h = \mathbf{v}_h + \nabla p_h$ and we decompose $\mathbf{v}_h = \sum_{i=1}^{N} v_i$ and $p_h = \sum_{i=N+1}^{N+M} p_i$ then we get

$$(4.2) \qquad\qquad (R_h^{-1}\mathbf{w}_h, \mathbf{w}_h) \le c\, h^{-2}(\|\mathbf{v}_h\|_0^2 + \|p_h\|_0^2).$$

5. THE MAIN THEOREM

We prove the main theorem estimating the condition number of the preconditioned system corresponding to the proposed two-level method in this section. We start with the following theorem proved in [15]. Its proof was based on the decomposition (cf. [12, 18]) of functions in $\mathbf{H}_0(\Omega; \text{curl})$ into a function in $\mathbf{H}_0^1(\Omega)$ and a gradient of a function in $H_0^1(\Omega)$.

Theorem 5.1. *A function* $\mathbf{u}_h \in \mathbf{Q}_h$ *can be decomposed as*

$$(5.1) \qquad\qquad \mathbf{u}_h = \mathbf{v}_h + \mathbf{\Pi}_h^Q \mathbf{z}_h + \nabla p_h,$$

where $\mathbf{v}_h \in \mathbf{Q}_h$, $\mathbf{z}_h \in \mathbf{S}_h$, $p_h \in S_h$ *satisfy*

$$h^{-1}\|\mathbf{v}_h\|_0 + \|\mathbf{z}_h\|_1 + \|\nabla p_h\|_0 \le C \|\mathbf{u}_h\|_{\mathbf{H}(\Omega; \text{curl})}$$

Using the above theorem and earlier results, we get our main result.

Theorem 5.2. *There are constants c and C independent of h satisfying*

$$c_1 A(\mathbf{u}, \mathbf{u}) \le A(\widetilde{B}_h A_h \mathbf{u}, \mathbf{u}) \le c_2 A(\mathbf{u}, \mathbf{u}), \quad \text{for all } \mathbf{u} \in \mathbf{Q}_h.$$

Proof. The above inequality is equivalent to

$$(5.2) \qquad c_2^{-1} A(\mathbf{u}_h, \mathbf{u}_h) \le (\widetilde{B}_h^{-1}\mathbf{u}_h, \mathbf{u}_h) \le c_1^{-1} A(\mathbf{u}_h, \mathbf{u}_h) \quad \text{for all } \mathbf{u}_h \in \mathbf{Q}_h.$$

For the first inequality, we have

$$A(\mathbf{v}_h, \mathbf{v}_h) \le 2(A(\mathbf{w}_h, \mathbf{w}_h) + A(\mathbf{\Pi}_h^Q \mathbf{v}_H, \mathbf{\Pi}_h^Q \mathbf{v}_H))$$

where we have decomposed $\mathbf{v}_h$ as in (2.5). The first inequality in (5.2) then follows from (4.1) and Corollary 3.1.

For the other direction, we start from the decomposition (5.1). We note that one can choose $\mathbf{z}_H \in \mathbf{S}_H$ and $p_H \in S_H$ such that for $H \simeq h$,

$$(5.3) \qquad \begin{aligned} h^{-1}\|\mathbf{z}_h - \mathbf{z}_H\|_0 + \|\mathbf{z}_H\|_1 &\le C\|\mathbf{z}_h\|_1\,, \\ h^{-1}\|p_h - p_H\|_0 + \|p_H\|_1 &\le C\|p_h\|_1\,. \end{aligned}$$

We illustrate the case of p_H as that of $\mathbf{z}_H$ is identical. Let $\bar{\Omega}_H = \cup T$, T in the H-mesh, $T \cap \Omega \neq 0$. Let $\widetilde{p}_H$ denote interpolant of p_h (extended by zero outside of Ω) with respect to the extended H-grid on $\bar{\Omega}_H$. We define p_H to be $\widetilde{p}_H$ on the interior vertices of Ω_H and set $p_H(v_i) = 0$ on the vertices of $\partial \Omega_H$. Now (3.3) holds with h and H interchanged (using the extended H-mesh). Thus, by the triangle inequality, (5.3) will follow if we show that

$$h^{-1}\|\widetilde{p}_H - p_H\|_0 + \|\widetilde{p}_H - p_H\|_1 \leq C\|\widetilde{p}_H\|_{1,\bar{\Omega}_H}.$$

Note that $\widetilde{p}_H - p_H$ lives on the H-elements which intersect $\partial \Omega_H$ and $\widetilde{p}_H$ vanishes on $\partial \bar{\Omega}_H$. Let $\{\varphi_i^{(H)}\}$ be the standard nodal piecewiese linear basis functions associated with the extended $\mathcal{T}_H$ mesh. Then,

$$\widetilde{p}_H - p_H = \sum_{v_i \in \partial \Omega_H} \widetilde{p}_H(v_i)\varphi_i^{(H)}.$$

The above sum is taken over vertices v_i on $\partial \Omega_H$. Then, since $\widetilde{p}_H$ vanishes on $\partial \bar{\Omega}_H$ it is clear that for the strip formed by the H-elements bordering $\partial \Omega_H$ one has,

$$h^{-2}\|\widetilde{p}_H - p_H\|_0^2 + \|\widetilde{p}_H - p_H\|_1^2 = h^{-2}\|\widetilde{p}_H - p_H\|_{0,\ \text{strip}}^2 + \|\widetilde{p}_H - p_H\|_{1,\ \text{strip}}^2$$

$$\leq CH \sum_{v_i \in \partial \Omega_H} \widetilde{p}_H(v_i)^2 \leq C\|\widetilde{p}_H\|_{1,\ \text{strip}}^2.$$

We then write

$$\mathbf{u}_h = \mathbf{v}_h + \mathbf{\Pi}_h^Q(\mathbf{z}_h - \mathbf{\Pi}_H^Q\mathbf{z}_H) + \nabla(p_h - \Pi_h^S p_H) + \mathbf{\Pi}_h^Q\mathbf{u}_H \,,$$

where $\mathbf{u}_H = \mathbf{\Pi}_H^Q\mathbf{z}_H + \nabla p_H$.

Using (5.3) with (3.3) gives

(5.4) $$\|p_h - \Pi_h^S p_H\|_0 \leq Ch\,\|\nabla p_h\|_0 \leq Ch\|\mathbf{u}_h\|_{\mathbf{H}(\Omega;\text{curl})}.$$

We next bound the term $\mathbf{\Pi}_h^Q(\mathbf{z}_h - \mathbf{\Pi}_H^Q\mathbf{z}_H)$. The problem is that we do not know that $\mathbf{\Pi}_h^Q$ is stable in $\mathbf{L}^2(\Omega)$ when applied to such a function. Set $\mathbf{C}$ to be the mean value of $\mathbf{z}_h$ on $\widehat{K}$ if $\widehat{K} \cap \partial \Omega = \emptyset$, otherwise, set $\mathbf{C} = \mathbf{0}$. As in (3.2),

$$\|\mathbf{z}_h - \mathbf{C}\|_{0,\widehat{K}} \leq Ch\|\mathbf{z}_h\|_{1,\widehat{K}}.$$

Then,

$$\|\mathbf{\Pi}_h^Q(\mathbf{z}_h - \mathbf{\Pi}_H^Q\mathbf{z}_H)\|_{0,K} = \|\mathbf{\Pi}_h^Q(\mathbf{z}_h - \mathbf{C}) + \mathbf{\Pi}_h^Q\mathbf{\Pi}_H^Q(\mathbf{z}_H - \mathbf{C})\|_{0,K}$$

$$\leq C\left(\|\mathbf{z}_h - \mathbf{C}\|_{0,\widehat{K}} + \|\mathbf{\Pi}_Q^H(\mathbf{z}_H - \mathbf{C})\|_{0,\widehat{K}} \right)$$

where we used the triangle inequality, (3.5) and Theorem 3.1 for the last inequality above. Now, $\mathbf{z}_h - \mathbf{C}$ is a continuous piecewise polynomial on the H-mesh (and vanishes on $\partial \Omega$ when $\widehat{K} \cap \partial \Omega \neq \emptyset$) so it follows that

$$\|\mathbf{\Pi}_Q^H(\mathbf{z}_H - \mathbf{C})\|_{0,\widehat{K}} \leq C\|\mathbf{z}_H - \mathbf{C}\|_{0,\widehat{K}} \leq \|\mathbf{z}_H - \mathbf{z}_h\|_{0,\widehat{K}} + \|\mathbf{z}_h - \mathbf{C}\|_{0,\widehat{K}}.$$

Combining the above estimates with limited overlap gives

$$\|\mathbf{\Pi}_h^Q(\mathbf{z}_h - \mathbf{\Pi}_H^Q\mathbf{z}_h)\|_0 \leq Ch\|\mathbf{z}_h\|_1 \leq Ch\|\mathbf{u}_h\|_{\mathbf{H}(\Omega;\text{curl})}.$$

Finally,

$$\|\mathbf{u}_H\|_{\mathbf{H}(\Omega;\mathrm{curl})} \leq CA(\mathbf{u}_h, \mathbf{u}_h)$$

follows from the triangle inequality, (3.6), (5.3) and Theorem 5.1.

The theorem follows from (2.5) and (4.2) taking $\mathbf{u}_H$ as above and $\mathbf{w}_h = \mathbf{v}_h + \mathbf{\Pi}_h^Q(\mathbf{z}_h - \mathbf{\Pi}_H^Q\mathbf{z}_H) + \nabla(p_h - \Pi_h^S p_H)$. $\square$

Remark 5.1. *The above proof actually showed that the component $\mathbf{u}_H$ can be chosen as an image of $\mathbf{z}_H$ (under $\mathbf{\Pi}_H^Q$) from the H^1–conforming space $\mathbf{S}_H$ plus a gradient of a function in S_H. This fact allows us to derive stable multilevel decompositions based only on conforming finite element functions defined on a hierarchy of meshes $\mathcal{T}_{H_k}$, $k = 1, 2, \ldots, J$. Here the finest auxiliary mesh $\mathcal{T}_H$ corresponds to $H = H_J$. Moreover, the components of the decomposition can be chosen so that they vanish on $\partial\Omega$. Details about such H^1–conforming multilevel decompositions based on nested spaces are found in Section 6 of [4]. Exploring this fact can lead to a proof of the optimal convergence of the multilevel method using the Hiptmair smoother, resulting from nested Nédélec spaces Q_{H_k}, $k = 1, 2, \ldots, J$, supported in Ω. Further details will not be presented here. We only illustrate the performance of such a multilevel method in Section 7.*

6. Proof of Theorem 3.1

6.1. **Commutativity.** Here we consider only lowest order spaces ($r = 0$) S_h, $\mathbf{Q}_h$, $\mathbf{R}_h$ and their counterparts with indices H. The techniques extend easily to higher order spaces. In what follows, $\boldsymbol{\tau}$ and $\mathbf{n}$ (possibly with subscripts) will denote unit tangential directions along edges and unit normal vectors to faces, respectively, in the tetrahedral meshes.

Since functions in S_H are continuous, the operator Π_h^S is well defined there. The degrees of freedom for $\mathbf{\Pi}_h^Q$ involve integrals of the tangential components along edges of the mesh $\mathcal{T}_h$. These integrals are obviously well defined for edges which are not tangent to any face of $\mathcal{T}_H$ as functions in $\mathbf{Q}_H$ are piecewise polynomial on such an edge with only point discontinuities. The integrals are well defined along edges when they are tangent to faces of $\mathcal{T}_H$ because the tangential component of a function in $\mathbf{Q}_H$ is continuous there. Similar arguments show that $\mathbf{\Pi}_h^R$ is well defined on $\mathbf{R}_H$.

Let u be in S_H. To check that $\nabla\Pi_h^S u = \mathbf{\Pi}_h^Q\nabla u$ we need only check that they have the same degrees of freedom since they are both in $\mathbf{Q}_h$. Consider an edge ℓ in the mesh $\mathcal{T}_h$ with end points v_1 and v_2 and let $\boldsymbol{\tau}_\ell$ be a unit vector pointing from v_1 to v_2. One has,

$$\int_\ell \nabla\left(\Pi_h^S u\right) \cdot \boldsymbol{\tau}_\ell \, ds = (\Pi_h^S u)(v_2) - (\Pi_h^S u)(v_1) = u(v_2) - u(v_1),$$

while

$$\int_\ell \mathbf{\Pi}_h^Q(\nabla u) \cdot \boldsymbol{\tau}_\ell \, ds = \int_\ell \nabla u \cdot \boldsymbol{\tau}_\ell \, ds = \sum_{K_H \cap \ell} \int_{\ell \cap K_H} \nabla u \cdot \boldsymbol{\tau}_\ell \, ds$$

$$= \sum_{[w_1, w_2] = K_H \cap \ell} (u(w_2) - u(w_1)) = u(v_2) - u(v_1).$$

We used the fact that u is continuous and that ℓ can be represented as a connected path of line segments $[w_1, w_2] = K_H \cap \ell$.

We check next that $\nabla \times \mathbf{\Pi}_h^Q \mathbf{u}$ and $\mathbf{\Pi}_h^R (\nabla \times \mathbf{u})$ have the same degrees of freedom (in $\mathbf{R}_h$) for $\mathbf{u} \in \mathbf{Q}_H$. Stokes' Theorem gives that for any face F of the mesh $\mathcal{T}_h$,

$$\int_F \left(\nabla \times \mathbf{\Pi}_h^Q \mathbf{u} \right) \cdot \mathbf{n} \, dx = \int_{\partial F} \mathbf{\Pi}_h^Q \mathbf{u} \cdot \boldsymbol{\tau} \, ds = \int_{\partial F} \mathbf{u} \cdot \boldsymbol{\tau} \, ds.$$

On the other hand, by the definition of $\mathbf{\Pi}_h^R$, one has,

$$\int_F (\mathbf{\Pi}_h^R (\nabla \times \mathbf{u})) \cdot \mathbf{n} \, ds = \int_F (\nabla \times \mathbf{u}) \cdot \mathbf{n} \, ds$$

$$= \sum_{F \cap K_H} \int_{F \cap K_H} (\nabla \times \mathbf{u}) \cdot \mathbf{n} \, ds$$

$$= \sum_{F \cap K_H} \int_{\partial (F \cap K_H)} \mathbf{u} \cdot \boldsymbol{\tau} \, ds$$

We split the above boundary integrals into integrals along edge segments along the boundary of F and interior segments. Using the fact the $\mathbf{u} \cdot \boldsymbol{\tau}$ is continuous on any interior edge segment, it is clear that each such segment results in two canceling contributions. Thus,

$$\int_F (\mathbf{\Pi}_h^R (\nabla \times \mathbf{u})) \cdot \mathbf{n} \, ds = \int_{\partial F} \mathbf{u} \cdot \boldsymbol{\tau} \, ds$$

showing that $\nabla \times \mathbf{\Pi}_h^Q \mathbf{u}$ and $\mathbf{\Pi}_h^R (\nabla \times \mathbf{u})$ have the same degrees of freedom. This shows the commutativity properties claimed by Theorem 3.1.

6.2. L^2–**stability of** Π_h^S, $\mathbf{\Pi}_h^Q$ **and** $\mathbf{\Pi}_h^R$ **on** S_H, $\mathbf{Q}_H$ **and** $\mathbf{R}_H$**.** Consider first Π_h^S. Let $\{x_i\}$ and $\{v_i\}$ denote, respectively, the vertices of $\mathcal{T}_h$ and $\mathcal{T}_H$. Let $T_H(x_i)$ denote a tetrahedron of $\mathcal{T}_H$ containing x_i. For $v_H \in S_H$, by quasi-uniformity,

$$\|\Pi_h^S v_H\|_0^2 \le Ch^3 \sum_{x_i} v_H(x_i)^2$$

$$\le Ch^3 \sum_{x_i} \sum_{v_j \in T_H(x_i)} v_H(v_j)^2 \le C \|v_H\|_0^2.$$

For the last inequality above, we used the fact that there are at most a fixed number (independent of h) of vertices from the h mesh in any element of the H mesh.

Consider next $\mathbf{\Pi}_h^Q$. Let K be a tetrahedron of $\mathcal{T}_h$ and B_K denote the Jacobian of the affine transformation F_K which maps the reference tetrahedron $\overline{K}$ onto K. The restrictions of functions in $\mathbf{\Pi}_h^Q$ to the element K are mapped to functions in the Nédélec space on the reference element by the transformation

$$\mathbf{v} \to B_K^t (\mathbf{v} \circ F_K).$$

Moreover the degrees of freedom are mapped according to the formula

$$(\mathbf{\Pi}_h^Q \mathbf{v}) \circ F_K = B_K^{-t} \overline{\mathbf{\Pi}}^Q (B_K^t (\mathbf{v} \circ F_K)).$$

Here $\overline{\mathbf{\Pi}}^Q$ denotes the Nédélec interpolation operator on the reference element. The following norm equivalences are a consequence of the equivalence of norms on the reference space and scaling arguments:

$$\|\mathbf{u}_h\|_{L_\infty(K)} \simeq \left(\sum_{i=1}^{6} (\mathbf{u}_h(\mathbf{v}_i) \cdot \boldsymbol{\tau}_i)^2 \right)^{1/2} \simeq h^{-3/2} \|\mathbf{u}_h\|_{0,K}.$$

Here we have used the notation $\simeq$ to denote norm equivalence with constants independent of h. Also, $\mathbf{v}_i$ is the center of the i'th edge e_i of K and $\boldsymbol{\tau}_i$ is the unit vector tangent to e_i.

Given $\mathbf{u}_H \in \mathbf{Q}_H$, one has,

$$\|\mathbf{\Pi}_h^Q \mathbf{u}_H\|_{0,K}^2 \simeq h^3 \sum_{i=1}^{6} \left(\frac{1}{|\ell_i|} \int_{\ell_i} \mathbf{u}_H \cdot \boldsymbol{\tau}_i \, ds \right)^2.$$

Moreover,

$$\frac{1}{|\ell_i|} \int_{\ell_i} |\mathbf{u}_H \cdot \boldsymbol{\tau}_i| \, ds = \frac{1}{|\ell_i|} \sum_{\ell_i \cap K_H} \int_{\ell_i \cap K_H} |\mathbf{u}_H \cdot \boldsymbol{\tau}_i| \, ds$$

$$\leq \sum_{\ell_i \cap K_H} \|\mathbf{u}_H\|_{L_\infty(K_H)}.$$

Since the number of elements K_H intersecting ℓ_i is bounded, one gets

$$\|\mathbf{\Pi}_h^Q \mathbf{u}_H\|_{0,K}^2 \leq C h^3 \sum_{\ell_i \cap K_H} \|\mathbf{u}_H\|_{L_\infty(K_H)}^2$$

$$\leq C h^3 \|\mathbf{u}_H\|_{L_\infty(\widehat{K})}^2$$

$$\leq C \|\mathbf{u}_H\|_{0,\widehat{K}}^2.$$

The L^2–stability of $\mathbf{\Pi}_h^Q$ follows by summation. The proof of the L^2–stability of $\mathbf{\Pi}_h^R$ is similar.

Remark 6.1. *The above proofs can be easily extended to other piecewise-polynomial spaces. For example, if $\mathbf{V}_H$ is a discrete space where $\mathbf{\Pi}_h^Q$ is well defined, then there exists $C > 0$ such that*

$$\|\mathbf{\Pi}_h^Q \mathbf{u}_H\|_0 \leq C \|\mathbf{u}_H\|_0$$

for any $\mathbf{u}_H \in \mathbf{V}_H$.

7. NUMERICAL EXPERIMENTS

In this section we present numerical results from experiments with different versions of the two-level preconditioner applied to the problem for $\mathbf{u} \in \mathbf{Q}_h$, such that for a given $\mathbf{f} \in \mathbf{L}^2(\Omega)$,

$$(\mathbf{u}, \, \mathbf{v}) + (\nabla \times \mathbf{u}, \, \nabla \times \mathbf{v}) = (\mathbf{f}, \, \mathbf{v}), \text{ for all } \mathbf{v} \in \mathbf{Q}_h.$$

Specifically, we considered:

(1) The multiplicative version of the preconditioner (2.2) with B_H being a $V(1,1)$ cycle of geometric multigrid (with Hiptmair smoothing) on the auxiliary mesh.

(2) The additive preconditioner (2.2) with geometric multigrid on the auxiliary mesh.

(3) The multiplicative preconditioner with exact solve on the auxiliary mesh.

(4) The additive preconditioner with exact solve on the auxiliary mesh ($\widetilde{B}_h$).

In all experiments we used the lowest order Nédélec space for computing the entries of A_h and F, with a right-hand side **1** and homogeneous boundary conditions. We also employed the multiplicative version of the Hiptmair smoother. The auxiliary mesh was chosen to be uniform, for the efficiency reasons addressed in Subsection 8.2.

We first present results in two dimension (see Subsection 8.1 for details). We chose two initial meshes on the unit square and used uniform refinement to generate larger problems, as shown in Figure 2. The refinement levels were synchronized such that the mesh size ratio is kept at approximately 1.06.
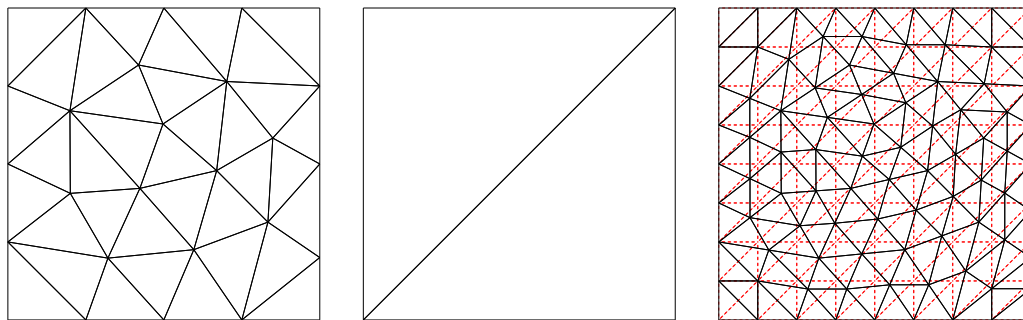

FIGURE 2. Initial mesh on the unit square (left), initial auxiliary mesh (center), and the composition of the two meshes after refinement (right).

Results of the preconditioned conjugate gradient iteration using the two-level preconditioners are reported in Table 1. The iterations were stopped after the norm of the initial residual was reduced by six orders of magnitude. The empty spots indicate that the execution time was too long. We use the following notation: ℓ is the refinement level of $\mathcal{T}_h$, N is the size of the problem in $\mathbf{Q}_h$. The same quantities for the auxiliary mesh are denoted with ℓ_{aux} and N_{aux}. In the last four columns we report the iteration count for each of the two-level preconditioners (1)-(4).

The results in Table 1 confirm that both the multiplicative and the additive versions lead to solution methods with bounded number of iterations. The additive preconditioner requires approximately twice as many iterations (but it is cheaper to compute). Another interesting observation is that using multigrid instead of exact solver on the auxiliary mesh, in both cases, leads to almost no increase in the number of iterations.

Next, we repeat the same experiment on an unstructured mesh on the unit cube, shown in Figure 3. As before, we refine both meshes, keeping the mesh size ratio at approximately 1.07.

ℓ	N	ℓ_{aux}	N_{aux}	n_1	n_2	n_3	n_4
0	62	2	56	4	8	3	8
1	232	3	208	4	9	4	9
2	896	4	800	4	9	4	9
3	3520	5	3136	4	9	3	8
4	13952	6	12416	4	8	3	8
5	55552	7	49408	4	8	3	7
6	221696	8	197120	4	7	3	7
7	885760	9	787456	4	7		
8	3540992	10	3147776	4	7		

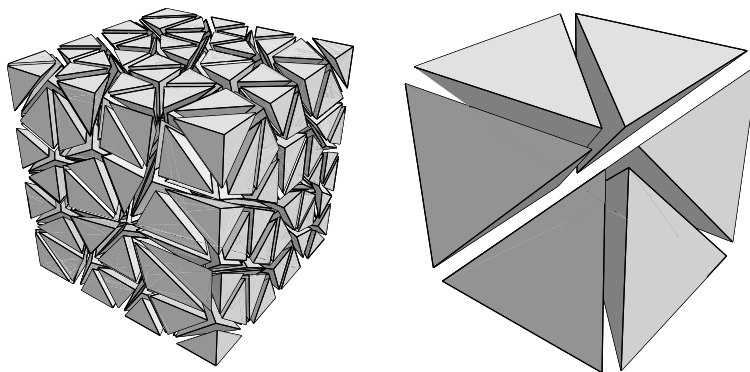TABLE 1. Numerical results for the problem on the unit square.

FIGURE 3. Initial mesh on the unit cube (left) and initial auxiliary mesh (right).

The behavior of the two-level preconditioners is presented in Table 2 and is similar to the two dimensional case.

ℓ	N	ℓ_{aux}	N_{aux}	n_1	n_2	n_3	n_4
0	722	2	604	4	9	4	9
1	5074	3	4184	5	10	4	10
2	37940	4	31024	6	16	5	16
3	293224	5	238688	6	16	6	15
4	2305232	6	1872064	6	16		

TABLE 2. Numerical results for the problem on the unit cube.

Again, we have a bounded number of iterations, with the additive count being approximately twice larger. As in Table 1, using multigrid instead of exact solve increases the number of iterations, at most, by one.

In the next set of examples, we allow for the auxiliary mesh to be defined on a domain Ω_H, that differs from the original domain Ω. This situation is of practical interest, since it allows for a problem defined on a very complicated mesh to be preconditioned by geometric multigrid on a box. Similar approaches for second order elliptic problems have been known as "fictitious" domain, or domain embedding methods and can lead to optimal multigrid preconditioners, see [20].

To demonstrate the algorithm, we set to precondition our discrete problem posed on a simple triangular domain, by using the uniform auxiliary mesh from our first experiment. On each refinement level, we define Ω_H by removing all elements of the auxiliary mesh that are not inside Ω. The process is illustrated in Figure 4. Since $\Omega_H \subset \Omega$, we get a sequence of nested auxiliary subspaces of $\mathbf{H}_0(\Omega; \mathrm{curl})$, for which we define our geometric multigrid preconditioner (based on Hiptmair smoothing). One simple way to implement this in practice is to eliminate all degrees of freedom corresponding to the removed elements from the stiffness matrices and all interpolation and smoothing operators.
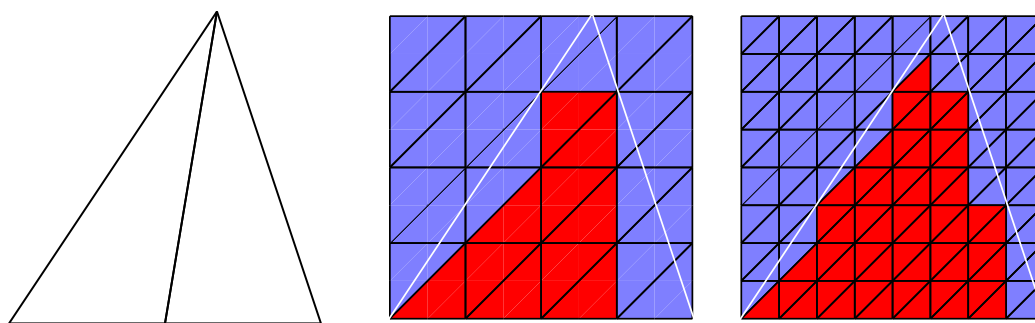

FIGURE 4. Initial mesh on the triangular domain and two auxiliary meshes inscribed in it.

The results for the so defined non-matching auxiliary mesh preconditioner are listed in Table 3. One observes that the number of iterations is larger than in the previous 2D experiment, but it eventually stabilizes. Compared to the earlier results, the gap between the two-level and the multigrid methods is larger.

ℓ	N	ℓ_{aux}	N_{aux}	n_1	n_2	n_3	n_4
4	800	4	800	10	17	8	16
5	3136	5	3136	11	19	8	16
6	12416	6	12416	12	20	8	16
7	49408	7	49408	12	20	7	15
8	197120	8	197120	13	20	7	14
9	787456	9	787456	13	20		
10	3147776	10	3147776	13	20		

TABLE 3. Numerical results for the problem on the triangular domain.

Our last test is a non-matching auxiliary mesh example in 3D where Ω is the reference tetrahedron, with vertices $(0,0,0)$, $(1,0,0)$, $(0,1,0)$ and $(0,0,1)$, split into eight elements. We used the uniform auxiliary mesh from the second example. The two meshes were refined such that the mesh size ratio on each level is approximately 1.10. The initial mesh and two auxiliary meshes Ω_H are shown in Figure 5.
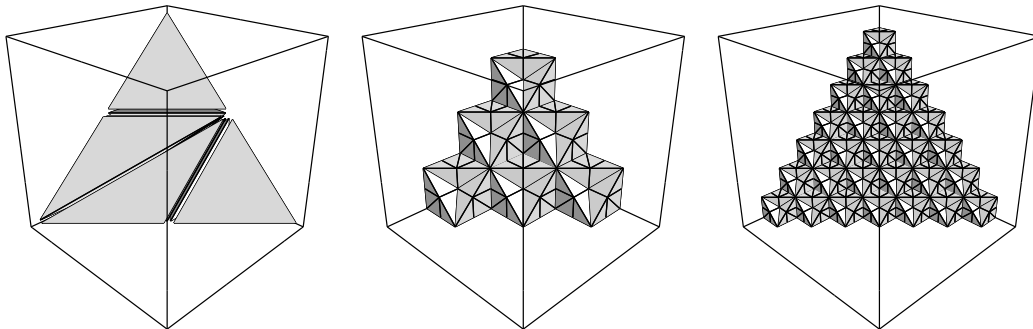

FIGURE 5. Initial mesh on the tetrahedral domain and two auxiliary meshes inscribed in it.

The numerical results in Table 4 suggest that, as with the previous test, the non-matching auxiliary mesh preconditioner requires more iterations and more refinement levels to exhibit its asymptotic behavior. In this case, the multiplicative methods performed significantly better than the additive ones. Finally, while the two level methods seem to be optimal, the number of iterations for the first two preconditioners are slightly increasing.

ℓ	N	ℓ_{aux}	N_{aux}	n_1	n_2	n_3	n_4
2	804	2	604	10	20	10	20
3	5576	3	4184	14	33	13	32
4	41360	4	31024	16	40	14	37
5	318240	5	238688	18	45	14	40
6	2496064	6	1872064	19	46		

TABLE 4. Numerical results for the problem on the reference tetrahedron.

8. Concluding Remarks.

8.1. **Two dimensional problems.** Even though we concentrated on the 3D case, the theory of the preceding sections can be modified such that the results hold for two dimensional problems. Below we outline how this can be done.

Assume that Ω is a convex polygonal domain, discretized with a triangular mesh. One defines $\mathbf{H}(\Omega; \mathrm{curl})$ as

$$\mathbf{H}(\Omega; \mathrm{curl}) = \{\mathbf{u}^{\perp} \ : \ \mathbf{u} \in \mathbf{H}(\Omega; \mathrm{div})\},$$

where $\mathbf{u}^{\perp} = (-u_2, u_1)$ is the $\frac{\pi}{2}$ rotation of the vector field $\mathbf{u} = (u_1, u_2)$. Furthermore, $\nabla \times \mathbf{u}^{\perp}$ is defined to be $\nabla \cdot \mathbf{u}$, and the Nédélec space $\mathbf{Q}_h$ keeps its definition provided we consider $\mathbf{x} \in \mathbb{R}^2$. The properties of the Hiptmair smoother are well known in 2D. The stable decomposition (5.1) also holds in this case, see [15]. Thus, the proof of Theorem 5.2 needs no changes, as long as the estimate

$$(8.1) \qquad \qquad \|\nabla \times \mathbf{\Pi}_h^Q \mathbf{u}\|_0 \le C \|\nabla \times \mathbf{u}\|_0$$

from Corollary 3.1 is available.

Since the right half of the commuting diagram (3.1) is defined only in 3D, we prove the above estimate directly. Fix $K \in \mathcal{T}_h$ and $\mathbf{u} \in \mathbf{Q}_H$. Then

$$\int_K \nabla \times \mathbf{\Pi}_h^Q \mathbf{u} \, dx = \int_{\partial K} \mathbf{\Pi}_h^Q \mathbf{u} \cdot \boldsymbol{\tau} \, ds = \int_{\partial K} \mathbf{u} \cdot \boldsymbol{\tau} \, ds = \int_K \nabla \times \mathbf{u} \, dx \, .$$

For the lowest order Nédélec space, $\nabla \times \mathbf{\Pi}_h^Q \mathbf{u}$ is a constant in K, so

$$\|\nabla \times \mathbf{\Pi}_h^Q \mathbf{u}\|_{0,K}^2 = \frac{1}{\mu(K)} \left(\int_K \nabla \times \mathbf{u} \, dx \right)^2 \le \|\nabla \times \mathbf{u}\|_{0,K}^2 \, ,$$

where $\mu(K)$ is the measure of K. This completes the proof of (8.1), and therefore we can conclude that our main results hold in two dimensions.

8.2. **Efficient implementation of $\mathbf{\Pi}_h^Q$.** The only non-standard part of the solution algorithm is the computation of the matrix representation of $\mathbf{\Pi}_h^Q$. This requires that for every basis function $\boldsymbol{\varphi}$ of $\mathbf{Q}_H$ one evaluates and stores the integrals $\int_\ell \boldsymbol{\varphi} \cdot \boldsymbol{\tau}_l \, ds$ over all edges ℓ of $\mathcal{T}_h$. In order to keep optimal complexity, this has to be done only for the integrals that are not zero, i.e. only for edges ℓ belonging to elements in $\mathcal{T}_h$ which intersect the support of $\boldsymbol{\varphi}$. Thus, an efficient implementation requires that we have a relation table, **AuxElement_Element**, which for each (auxiliary) element in $\mathcal{T}_H$ gives the list of elements in $\mathcal{T}_h$ that intersect it. In practice, it might be easier to construct the above relation table (implemented as a boolean sparse matrix, for example) as the transpose of the similar **Element_AuxElement**. In particular, if the auxiliary mesh is uniform, one can directly enumerate all auxiliary elements intersecting, e.g., the bounding box of a given element in $\mathcal{T}_h$, since the auxiliary vertices form a simple lattice. If the auxiliary mesh is not uniform, the computation of **AuxElement_Element** becomes much more involved, and should probably be incorporated in the mesh generation process, in order to achieve optimal complexity.

REFERENCES

[1] C. Amrouche, C. Bernardi, M. Dauge, and V. Girault. Vector potentials in three-dimensional non-smooth domains. *Math. Methods Appl. Sci.*, 21(9):823–864, 1998.

[2] D. N. Arnold, R. S. Falk, and R. Winther. Multigrid in *H*(div) and *H*(curl). *Numer. Math*, January 2000. Published online, DOI 10.1007/s002110000137.

[3] G. Astrakhantsev. Method for fictitious domains for a second-order elliptic equation with natural boundary conditions. *U.S.S.R. Comp. Math. and Math. Phys.*, 18:114–121, 1978.

[4] J. H. Bramble. *Multigrid Methods*. Number 294 in Pitman research notes in mathematics series. Longman Scientific & Technical, Harlow, UK, 1993.

[5] J. H. Bramble, J. E. Pasciak, and X. Zhang. Two-level preconditioners for 2m'th order elliptic finite element problems. *East-West Jour. Numer. Math.*, 4:99–120, 1996.

[6] S. Brenner and L. Scott. *The Mathematical Theory of Finite Element Methods.* Springer-Verlag, New York, 1994.

[7] S. C. Brenner. Preconditioning complicated finite elements by simple finite elements. *SIAM J. Sci. Comput.*, 17(5):1269–1274, 1996.

[8] F. Brezzi and M. Fortin. *Mixed and Hybrid Finite Element Methods.* Springer-Verlag, New York, 1991.

[9] B. Buzbee, F.W. Dorr, J.A. George, and G.H. Golub. The direct solution of the discrete poisson equation on irregular regions. *SIAM J. Numer. Anal.*, 8:722–736, 1971,.

[10] V. Girault and P. Raviart. *Finite Element Approximation of the Navier-Stokes Equations.* Lecture Notes in Math. # 749, Springer-Verlag, New York, 1981.

[11] R. Hiptmair. Multigrid method for Maxwell's equations. *SIAM J. Numer. Anal.*, 36(1):204–225, 1999.

[12] R. Hiptmair. Finite elements in computational electromagnetism. *Acta Numer.*, 11:237–339, 2002.

[13] R. Hiptmair and A. Toselli. Overlapping Schwarz methods for vector valued elliptic problems in three dimensions. In *Parallel solution of PDEs*, IMA Volumes in Mathematics and its Applications. Springer–Verlag, Berlin, 1998.

[14] R. Hiptmair, G. Widmer, and J. Zou. Auxiliary space preconditioning in $H(curl)$. *Numer. Math.*, 103(3):435–459, 2006.

[15] R. Hiptmair and J. Xu. Nodal auxiliary space preconditioning in $H(curl)$ and $H(div)$ spaces. Technical Report 2006-09, ETH, Switzerland, 2006.

[16] T. V. Kolev and P. S. Vassilevski. Parallel H^1-based auxiliary space AMG solver for $H(curl)$ problems. Technical Report UCRL-TR-222763, LLNL, July, 2006.

[17] T. V. Kolev and P. S. Vassilevski. Some experience with a H^1-based auxiliary space AMG for $H(curl)$ problems. Technical Report UCRL-TR-221841, LLNL, June, 2006.

[18] J. Pasciak and J. Zhao. Overlapping Schwarz methods in H (curl) on polyhedral domains. *J. Numer. Math.*, 10:221–234, 2002.

[19] B. F. Smith, P. E. Bjørstad, and W. D. Gropp. *Domain Decomposition. Parallel Multilevel Methods for Elliptic Partial Differential Equations.* Cambridge University Press, Cambridge, 1996.

[20] J. Xu. The auxliary space method and optimal preconditioning techniques for unstructured grids. *Computing*, 56:215–235, 1996.

CENTER FOR APPLIED SCIENTIFIC COMPUTING, UC LAWRENCE LIVERMORE NATIONAL LABORATORY, P. O. BOX 808, L-560, LIVERMORE, CA 94551, USA.
E-mail address: `tzanio@llnl.gov`

DEPARTMENT OF MATHEMATICS, TEXAS A & M UNIVERSITY, COLLEGE STATION, TX 77843-3368, USA.
E-mail address: `pasciak@math.tamu.edu`

CENTER FOR APPLIED SCIENTIFIC COMPUTING, UC LAWRENCE LIVERMORE NATIONAL LABORATORY, P. O. BOX 808, L-560, LIVERMORE, CA 94551, USA.
E-mail address: `panayot@llnl.gov`